Chemical and Process Engineering: New Frontiers, 2025, 46(4), e117
DOI: 10.24425/cpe.2025.155555

Utilization of 3D printing technology to prepare foam fractionation columns to separate saponins from *Sapindus mukorossi*

Mateusz Sochacki[1*], Piotr Michorczyk[2], Otmar Vogt[2], Marcin Piotrowski[2]

[1] Cracow University of Technology, CUT Doctoral School, Faculty of Chemical Engineering and Technology, Warszawska 24, Cracow 31-155, Poland
[2] Cracow University of Technology, Faculty of Chemical Engineering and Technology, Warszawska 24, Cracow 31-155, Poland

*** Corresponding author, e-mail:**
mateusz.sochacki@doktorant.pk.edu.pl

Article info:
Received: 21 July 2025
Revised: 23 October 2025
Accepted: 19 November 2025

Abstract
Biosurfactants carry many environmental benefits while providing similar properties to their synthetic counterparts. Due to their problematic production, efficient technologies for the separation of biosurfactants from aqueous solutions are being sought. Current work utilizes foam fractionation of saponins in a single and two-stage batch mode using a fully 3D printed separation column. The single stage column enriched saponin concentration from 0.062 to 3.008 mg/cm^3, which corresponds to enrichment ratio and recovery percentage of 48.23 and 16.00%, respectively. Under optimal operating conditions, the two-stage mode enabled the separation of saponins, reaching total percentage recovery of 71.63% which is significantly more than the one-stage mode alone. The enriched product was subjected to FT-IR, UV-vis and HPLC UV-vis/DAD analysis, proving the content of cyclic and acyclic glycosides. 3D printing technology provided a suitable column capable of obtaining high enrichment ratio reaching over 100-fold increase in saponin concentration up to 7.043 mg/cm^3.

Keywords
foam fractionation, 3D printing, *Sapindus mukorossi*, washnut, saponin

1. INTRODUCTION

Surfactants consist of a diverse group of organic compounds, widely used in households and industry (Arora et al., 2022; Kumar Dutta, 2019). They are found in many consumer products, including laundry detergents, wetting agents, hygiene products, cosmetics, food, paper, paints and pharmaceuticals (Farn, 2006; Shaban et al., 2020). Their negative impact on the environment is due to the residual release into the environment via improper treatment of wastewater, followed by accumulation in soil, water or sludge (Badmus et al., 2021; Ivanković and Hrenović, 2010; Kaczerewska et al., 2020). The rising global consumption of surfactants is increasing every year, thus some preventive measures are required to protect the environment from the increasing amount of produced surfactant waste.

Saponins represent a group of biosurfactants that exhibit significantly lower environmental impact compared to their synthetic counterparts and are viewed as a natural, renewable and biodegradable alternative (Hayes and Smith, 2019; Hojnik et al., 2019; Khan, 2018; Kharissova et al., 2019; Myers, 2020). Saponins belong to the group of biosurfactant glycosides, structurally consisting of a hydrophobic aglycone (genin) and hydrophilic sugar chains (glycone) synthesized by plants and some marine organisms (Moses et al., 2014; Stochmal et al., 2008). As a result of varying polarity within the given molecule, these glycosides exhibit surface-active properties, strong foamability and a wide range of biological activities that include anti-inflammatory, antipyretic, antibacterial, antifungal or anticancer properties (Bartnik and Facey, 2017; Sochacki and Vogt, 2022). Conventional isolation methods of saponins are problematic, time-consuming and expensive due to the need for specific apparatus and reagents (Majinda, 2012). This translates into low availability and a high cost of commercially available industrial-quality saponins. Consequently, new technologies that are also eco-friendly are being actively sought after.

A promising emerging technology is foam fractionation, which belongs to the adsorptive bubble separation methods .(Lemlich, 1968). Foam separation is distinguished as a simple and eco-friendly method for recovery or removal of numerous surface-active and inactive compounds (Backleh-Sohrt et al., 2005; Kumar and Ghosh, 2022; Srinet et al., 2017; Yang et al., 2011). The technology involves a controlled gas barbotage into the detergent solution, forcing surfactant adsorption and foam production. The aforementioned foam functions as a transport medium entrapping and transferring surfactant molecules from the initial solution, into enriched foamate (Stevenson, 2012; Stevenson and Li, 2014). The concentration of adsorbed material in the foam network is usually significantly greater in relation to the aqueous solution due to surfactant enrichment (Buckley et al., 2022). However, a proper selection of process parameters is required to achieve high efficiency at low process costs. In addition, foam frac-

tionation technology can be used in a variety of operating modes. The basic modes include batch and continuous modes, which operate with a depleting and continuously replenished foaming solution, respectively. Complex operating modes also include the use of additional streams for either or both reflux and stripping. Additionally, separation efficiency can be improved through the multi-stage system application (Burghoff, 2012; Lemlich, 1972; Sochacki et al., 2025).

In the past decade, a number of studies were published regarding the use of foam fractionation in saponin separation. Yan et al. (2011; 2012) conducted a number of studies on the separation of triterpenoid saponins from *Camellia sinensis* L. tea cake in batch and continuous two-stage modes. Jiang et al. (2016) fractionated triterpenoid saponins from soybean meal using a two-stage continuous mode. Wang et al. (2022) conducted a one-stage batch foam fractionation of dioscin from *Trigonella foenum-graecum* L. The study with the greatest impact was performed by Li et al. (2013) with the use of an internal spiral component (SIC) that improved the overall foam fractionation efficiency of saponins from *Sapindus mukorossi* Gaertn. In the two-stage batch mode, the authors obtained an enrichment and recovery equal to 133.4 and 36.4%, respectively, which are the best results obtained to date (Li et al., 2013).

Effective technologies for mass separation of saponins through foam fractionation are currently being developed. Such technologies require to maintain both a high enrichment ratio and total percentage recovery of saponins, which is hard to achieve. Designing foam fractionation columns is not a complicated task, but its minor improvements allow to significantly improve the overall process performance. A versatile tool for modeling complex and accurate systems with high quality is 3D printing technology. In the context of numerous studies on foam fractionation, no work has yet focused on the use of 3D printing for column designing, particularly for saponin separation purposes. In the current work, 3D designing and, printing technology was utilized to develop a foam fractionation column to separate triterpenoid saponin from pericarp of the *Sapindus mukorossi* fruits, which have been shown to be well suited for foam fractionation.

2. MATERIALS AND METHODS

2.1. Materials

Dried pericarps of *Sapindus mukorossi* Gaertn. (Nepal), were purchased from a local company (Grupa MTS Polska, Kraków). Reagents were purchased from the following manufacturers: methanol, isopropanol, ethanol 99.8%, sulfuric acid 95% (Chempur, Poland), vanillin 99% (Carl Roth), oleanolic acid 97% (Acros organics, China), acetonitrile LC-MS hypergrade (LiChrosolv Supelco), Mili-Q HPLC-grade purified water. Distilled water (1.1 µS/cm and 5.50 pH) was produced freshly before and used in each foam fractionation study. To manufacture the fractionation column elements, BD MICROLANCE mm injection needles (Medimall, Poland), Anycubic Basic Clear 1kg 3D Printing UV Sensitive Resin (405 nm) and Anycubic Photon M3 Max printer (Anycubic, China) were used.

2.2. Methods

2.2.1. Saponin extract preparation

Dried pericarps were grounded into a fine powder using an electric mill, then macerated for 24 h at room temperature in methanol at a ratio of 1:10 (g:cm^3), then further Soxhlet extracted for 4h using macerate as methanol at boiling point. The obtained extract was filtered through a G0 sintered glass filter and dried using rotary evaporator. A light orange powder with a sweet nutty odor was obtained. The extraction yield and the total saponin content were 80.12% and 22.87% wt., respectively.

2.2.2. Total saponin content assay

The assay was conducted using the vanillin - sulfuric acid colorimetric (Hiai et al., 1976; Le et al., 2018). The 0.5 cm^3 of sample, standard or blank was added to 0.5 cm^3 of 8% (m/v) vanillin solution in 99.8% ethanol and 5 cm^3 of 72% (v/v) aqueous sulfuric acid solution while cooling with cold water. The samples were incubated for 15 min at 60 °C while stirring, then cooled in cold water for 5 min. The maximum absorbance was determined by a sample scan within the 450–700 nm range. In this study oleanolic acid was used as standard, since it is structurally similar to the oleanolic type saponins present in the fruits (Sochacki and Vogt, 2022). Early data obtained for escin (560 nm) were normalized against oleanolic acid. The normalization constant was 1.15528. The maximum absorbance of the standard was located at 540 nm, close to the maximum of the tested samples (535 nm), and was chosen as the reference wavelength. The measurements were conducted using a Thermo Scientific Evolution 201/220 UV-Visible Spectrophotometer and quartz 1 cm thick cuvettes.

Standard calibration curve was prepared according to above procedure (Fig. 1). A stock solution of 0.25 mg/cm^3 oleanolic acid in absolute ethanol was prepared. The stock solution was diluted with ethanol to 0.20, 0.15, 0.10 and 0.05 mg/cm^3. Absorbance measurements were made at 540 nm against the reagent blank and repeated threefold. The mean value was used to plot the curve.

2.2.3. Column and sparger design

Digital models (CAD) of the column segments were prepared in SketchUp Free 3D design software. The column consisted of four elements: the lower segment, the middle segment, the upper segment and the barbotage disk. The individual segments

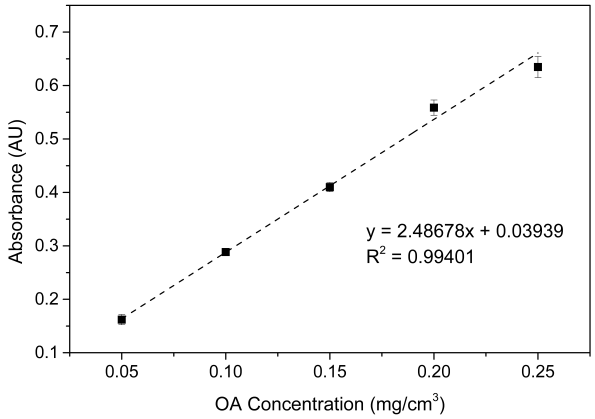

Figure 1. Oleanolic acid standard curve for total saponin content determination procedure.

are compatible and can be combined to form a full-fledged column of a given height. Models in .stl format were subjected to slicing in Anycubic Photon Workshop v2.2.19 x86 according to the adopted parameters in Table 1. Each component was printed in an Anycubic Photon M3 Max (DLP, digital light processing), cleaned in IPA, joined and sealed at the joints with universal silicone (Fig. 2 and Fig. 3). Additionally, before the column construction 24-pore disks were prepared by resin casting using standardized BD MICROLANCE needles with specific diameters. Before the actual trials the functionality of the column was verified.

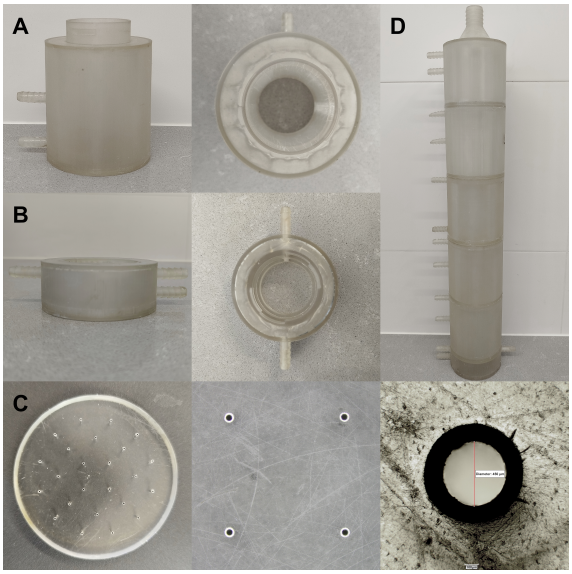

Figure 2. Printed column elements. A) middle segment, B) lower segment, C) sparging disc (450 µm), D) joined column.

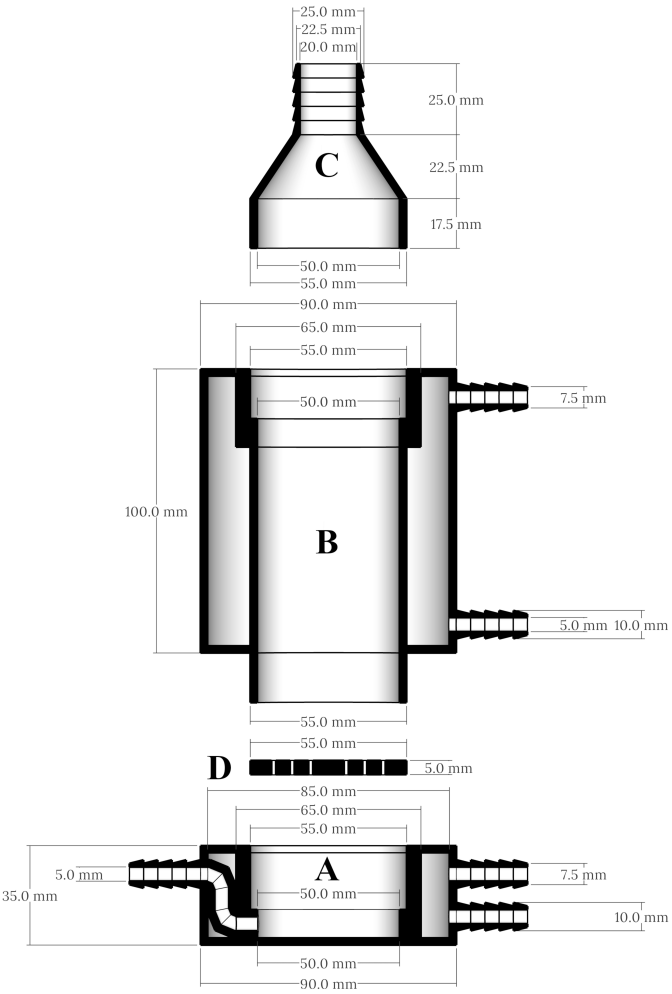

Figure 3. SketchUp.stl column elements. A) lower segment, B) middle segment, C) upper segment, D) sparging disc.

2.2.4. Foam fractionation procedure

The foam fractionation process was carried out in a semi-batch mode, according to the experimental setup in Fig. 4. The initial saponin solution was prepared by dissolving a measured amount of powdered extract in a given volume of distilled water. The solution was loaded into the column from the top with a funnel while feeding air into the column through the sparging disc. Each cycle was carried out until the generated foam was too unstable to reach the top of the column and be further extracted. Before the next cycle, the column was firmly rinsed and washed with distilled water, then the excess water was removed.

Table 1. Anycubic Photon M3 Max print parameters.

Normal exposure time [s]	Bottom exposure time [s]	Off time [s]	Bottom layers	Layer thickness [mm]	Anti-alias	Z-Lift distance [mm]	Z-Lift speed [mm/s]	Z Retract speed [mm/s]
8.0	30.0	4.0	7	0.05	1	10.0	4.0	4.0

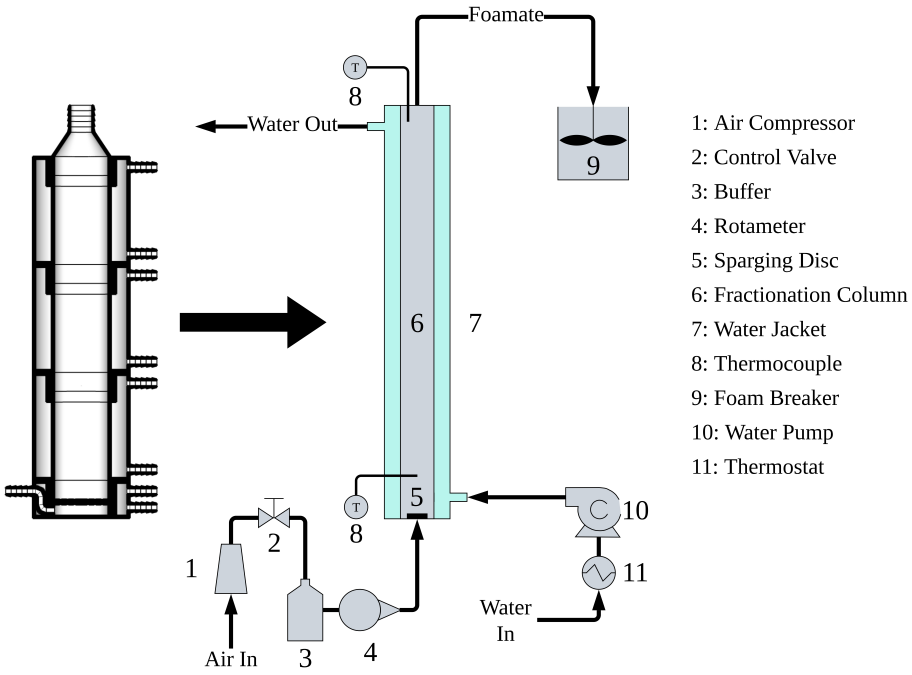

Figure 4. Schematic of the experimental setup.

The foam fractionation process was monitored and the process parameters were selected using the Simplex algorithm (1).

$$x_{ki} = \frac{2}{n}\left(\sum_{j=1}^{n+1} x_{kj} - x_{kq}\right) - x_{kq} \quad (1)$$

where x_{ki} introduces new process variable, x_{kj} is the sum of all investigated variables in the current set and x_{kq} is the variable that belongs to the lowest value of process efficiency. The process parameters screening is conducted with $n+1$ experiments, where n is the number of parameters screened. The parameters are entered into the formula in the appropriate order based on the process performance factor of individual experiments. The formula is used to calculate new parameters for the next experiment, which should improve selected process performance factor. If there is no improvement in performance, variables corresponding to additional experiments can be introduced into the equation to calculate other new parameters for the next experiment. The algorithm enables gradual improvement of the performance factor until a local maximum is reached.

The process efficiency was evaluated according to the performance factors: enrichment ration E in first stage (2) and recovery percentage R in the second stage (3).

$$E = \frac{C_f}{C_0} \quad (2)$$

$$R = \frac{C_f V_f}{C_0 V_0} \cdot 100\% \quad (3)$$

where C_f [mg/cm^3] is the foamate saponin concentration, C_0 [mg/cm^3] is the initial saponin concentration, V_f [cm^3] is the foamate volume, V_0 [cm^3] is the initial solution volume.

2.2.5. Product handling and analysis

The saponin concentration in foamate obtained in each cycle was conducted using TSC assay. The foamate was frozen and freeze-dried at –90 °C and 1 mbar for 12 h using Martin Christ Alpha 1-2 LDplus lyophilizer and kept at –20 °C until further analysis. Solid foamate was subjected to FTIR-ATR analysis within 4000–650 cm^{-1} using Nicolet^{TM} iS^{TM} 10 spectrophotometer, resolution of 4 cm^{-1} and 128 total scans in relation to oleanolic acid standard. The foamate was subjected to a HPLC UV-vis/DAD system analysis on Agilent (1100 Series), BDS Hypersil C_{18} column (250 × 4.6 mm, 5 µm, 120A) and separated with acetonitrile A/demineralized water (Mili-Q) B (A:B, 2:3 0 min, 4:1 20 min, 2:3 30 min) at flow rate of 1 cm^3/min, injection volume of 100 mm^3 and room temperature. The UV-detector was set at maximum absorption wavelength of 210 nm.

3. RESULTS AND DISCUSSION

3.1. 3D printed column performance

3.1.1. Effect of initial saponin concentration on column performance control

The effect of initial saponin concentration was investigated and ranged from 0.64 g/cm^3 to 0.064 mg/cm^3 (TSC) for constant variables of natural pH, volumetric air flow rate at 10 dm^3/h, 300 µm pore size, liquid volume of 500 cm^3, total column height of 100 cm and temperature (25 ± 1 °C). The results are shown in Fig. 5.

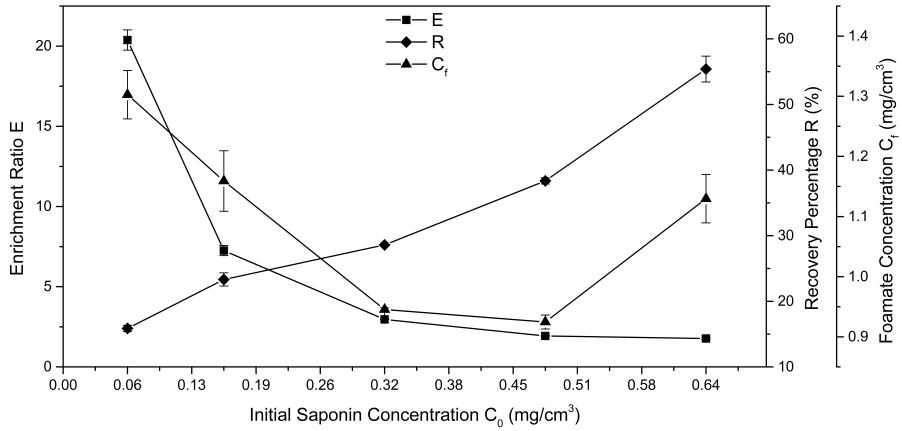

Figure 5. Effect of the initial saponin concentration on E, R, and C_f factors.

The main surface-active species in the *S. mukorossi* fruit extract are glycosides, mostly triterpenoid saponins and sesquiterpene (Heng et al., 2014; Ling et al., 2020). The effect of the initial saponin concentration is clearly visible. According to Stevenson and Li (2014) due to the increasing amount of surface-active species in the initial solution, a more stable foam is produced due to the amount of adsorbed saponins in the foam. Adsorbed surfactants slow the foam decay mechanism which include bubble coalescence and coarsening, increasing the liquid content in the foam (Bhakta and Ruckenstein, 1997; Stevenson and Li, 2014). The foam production process was observed. Foam bubble size distribution was uniform above concentration of 0.32 mg/dm^3, whereas foam decay effects started to occur below this value and the bubble size distribution began to change drastically with foam height. Frequent foam bubble bursting and prolonged foam discharge time were observed with decreasing initial saponin concentration. Bubble ruptures caused the release of interstitial liquid and appearance of internal reflux due to poor foam stability (Lemlich, 1968), drastically improving the enrichment ratio of saponins from 1.77 to 20.38 for 0.64 and 0.064 mg/cm^3, respectively. Another consequence of decreasing foam stability was the reduction of total saponin recovery from 55.40% to 15.86%, for the corresponding concentration values, as shown in Fig. 5. The sudden increase of foamate concentration at 0.64 mg/cm^3 can be explained by a significant increase in the initial saponin concentration. The saponins present in the foamate originate from the initial solution. The concentration relationship appears to be consistent with the literature (Jiang et al., 2016; Li et al., 2013).

3.1.2. Effect of volumetric air flow rate on column performance control

The effect of air flow rate was studied, since it is directly correlated with the processes of surfactant adsorption and foam formation (Wheaton et al., 1979). The air flow rate ranged from 5 to 25 dm^3/h at fixed parameters of natural pH, initial saponin concentration of 0.16 mg/dm^3, 300 µm pore size, liquid volume of 500 cm^3, total column height of 100 cm and temperature (25 ± 1 °C). The results are shown in Fig. 6.

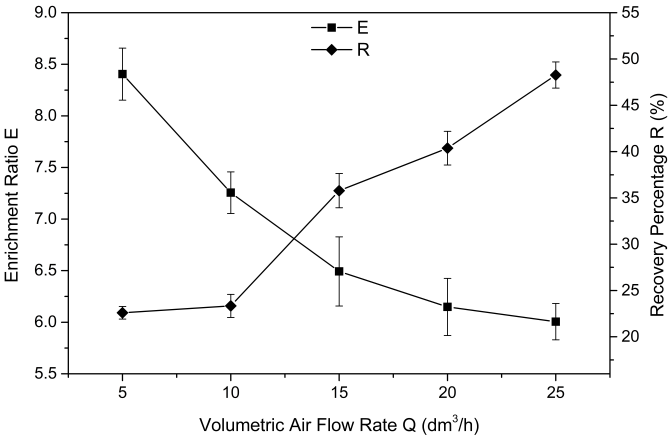

Figure 6. Effect of the volumetric air flow rate on E, R factors.

Air flow rate indicates the volume of gas introduced into the liquid pool and bubble-liquid contact time. The bubble residence time is increased as the air flow increases. Greater gas volume results in more surface area for molecular adsorption in the liquid pool. As a result of increased volumetric air flow rate, the foam residence time in the column is shortened. As expected, the enrichment ratio of saponins is slowly increased as the foam residence time decreases (Boonyasuwat et al., 2003). According to Fig. 6 at volumetric air flow rate of 5 dm^3/h the enrichment ratio reaches its maximum of 8.41-fold concentration increment and low 22.59% recovery of saponins. This value drops when the flow rate is increased to 25 dm^3/h as more volume of air is sparged into the solution, shortening foam residence time. Foam stability is improved as more surface-active material is present in the foam network, which weakens the foam drainage (Bharadwaj and Gupta, 2021). The wetter foam shows greater saponin recovery reaching 48.27% at lower enrichment ratio of 6.01. The results are similar to other studies regarding the impact of air flow rate on surfactant enrichment ration and recov-

ery percentage (Tharapiwattananon et al., 1996; Yan et al., 2011). As shown, the effect of the volumetric air flow rate has a stronger impact on the recovery than the enrichment ratio.

3.1.3. Effect of sparger pore size on column performance control

The effect of sparger pore size was evaluated via preparation of multiple 3D printed 24-pore discs. The designated pore sizes were 600, 450, 300, 230 and 180 µm obtained using 23G (outer 0.6 mm diameter), 26G (inner 0.23 mm and outer 0.45 mm diameter), 30G (inner 0.18 mm and outer 0.3 mm diameter) BD Microlance^{TM} 3 needles. The evaluation was carried out using a highly diluted solution at saponin concentration of 0.054 mg/dm^3. Other fixed parameters were natural pH, volumetric air flow rate at 50 dm^3/h, liquid volume of 500 cm^3, total column height of 100 cm and temperature ($25 \pm 1\,^{\circ}$C). The results are shown in Fig. 7.

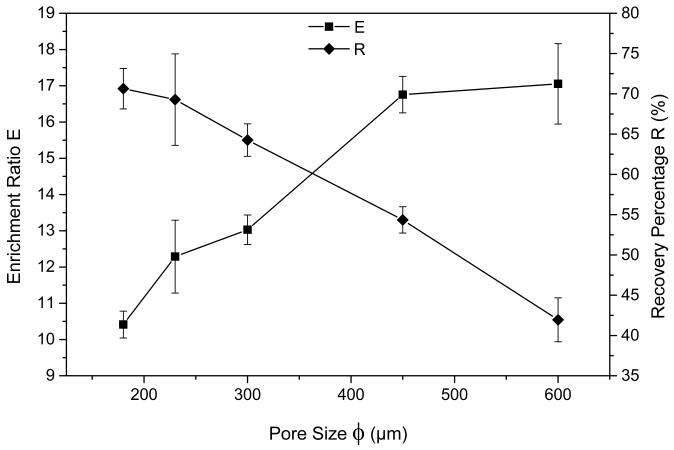

Figure 7. Effect of sparger pore diameter on E, R factors.

In addition to the gas flow rate, pore size of the sparger also affects the quality of produced foam through the size of produced bubbles. Gas-liquid surface area is directly related to interfacial adsorption. Smaller bubbles provide a greater surface area for adsorption, hence a more stable foam is often produced while decreasing bubble diameter. Larger bubbles produce foam cells with thinner film, which results in faster coalescence, ripening and ruptures (Du et al., 2001; Stevenson and Li, 2014). On the other hand, larger bubbles enhance foam drainage through the release of interstitial liquid creating non-uniform foam more susceptible to the effects of foam decay (Bhakta and Ruckenstein, 1997; Moradpour et al., 2024). Smaller bubble size can be easily achieved by reducing the sparger pore size, as shown in Fig. 7. At constant volumetric air flow rate, the increased gas pressure resulting from the reduction in pore size causes greater volume of bubbles introduced into the solution improving the bubble-liquid contact time. More adsorbed surfactant molecules provide a more stable foam, hence the decrease in pore size from 600 to 180 µm reduces the recovery percentage from 70.64 to 41.95%, but improves the enrichment ratio from 10.41 to 17.05, respectively. The results appear to be consistent with similar studies (Li et al., 2014; Tharapiwattananon et al., 1996). Despite the very high dilution of saponins, either high enrichment ratio or recovery percentage can be achieved.

3.1.4. Effect of column height on column performance control

The effect of column height was examined on recovery percentage and enrichment ratio of *S. mukorossi* saponins. This evaluation was performed at total column height ranging from 40 to 100 cm, and at fixed parameters of natural pH, initial saponin concentration of 0.064 mg/cm^3, 300 µm pore size, liquid volume of 500 cm^3 (which occupied 25 cm of total column height), volumetric air flow rate of 10 dm^3/h and temperature of $25 \pm 1\,^{\circ}$C. The results are shown in Fig. 8.

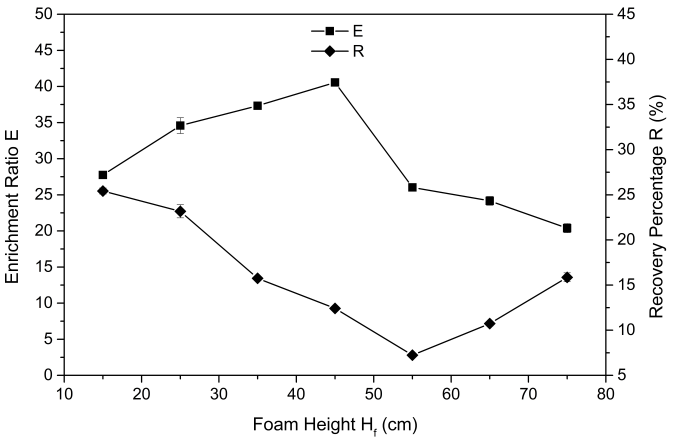

Figure 8. Effect of column height on E, R factors.

The typical influence of foam height has been studied by many authors, and implies an increase in enrichment ratio with increase in foam height. A natural result is also a decrease in total surfactant recovery (Boonyasuwat et al., 2003; Kumar and Ghosh, 2022; Sarachat et al., 2010). This effect is visible in Fig. 8 when the column height is reduced below 45 cm. The increase in the foam height and the foam residence time within the column results in improved foam drainage. Ultimately, it translates into more effective internal reflux, greater enrichment at the cost of reduced surfactant recovery. Typically, this process occurs to the point where the stability of the foam is insufficient enough and the column height is too great to achieve the foam overflow (Stevenson and Li, 2014). In the course of the study, it was observed that the method of loading the foaming liquid into the column affected the foam fractionation performance. The foaming liquid was poured from the highest point, which caused a sudden formation of foam above the liquid layer, due to the liquid impact on the column base. This layer caused stabilization of the newly produced form in the initial stage of the process. Below 45 cm of total column height, this effect was negligible. The saponin enrichment improved and reached maximum of 40.56, and the recovery reached value of 12.41%.

3.2. Two-stage foam fractionation technology

A two-stage batch-mode foam fractionation method was developed based on similar technologies used successfully in the purification of saponins (Jiang et al., 2016; Li et al., 2013; Yan et al., 2011). According to Fig. 9, the two-stage system enriches the saponins from the initial solution in the first column and recovers the remaining saponins from the depleted solution in the second column. Due to the substantial effect of process variables on the enrichment ratio and recovery percentage of saponins, operating parameters of each column were selected using Simplex method.

3.2.1. Simplex method of the first stage

First stage parameter screening was carried out in two steps. The first step was performed under fixed parameters of natural pH, 300 µm pore size, liquid volume of 500 cm^3, and temperature of 25 ± 1 °C. The second step was performed under fixed parameters of natural pH, 300 µm pore size, initial saponin concentration of 0.06 mg/cm^3, volumetric air flow rate of 10 dm^3/h and temperature of 25 ± 1 °C.

According to Table 2, the first step of parameter screening showed that the reduction in initial saponin concentration from 0.32 to 0.064 mg/cm^3 and volumetric air flow rate from 15 to 10 dm^3/h increased enrichment ratio to 20.38 and decreased recovery rate to 15.38%. In the second step, total column height and loading liquid volume were screened to further increase the enrichment ratio. The reduction in column height to 70 cm improved the enrichment ratio to 40.56 and reduced the recovery percentage to 12.41% (Table 3). Increase in loading liquid volume from to 500 cm^3 (25 cm) to 700 cm^3 (35 cm) resulted in increased bubble residence time and better surfactant adsorption. The foam stability was improved, hence greater liquid content, recovery percentage and lower saponin enrichment ratio due to loss of internal reflux. The reduction of liquid volume to 300 cm^3 (15 cm) prevented the foam overflow due to already insufficient foam stability, and reduced bubble residence time (Morgan and Wiesmann, 2001; Tharapiwattananon et al., 1996; Yan et al., 2011).

Ultimately the volume of 500 cm^3 appeared to be an appropriate operating volume. Other designated first stage parameters were initial saponin concentration of 0.064 mg/cm^3, 70 cm total column height and volumetric air flow rate of 10 dm^3/h.

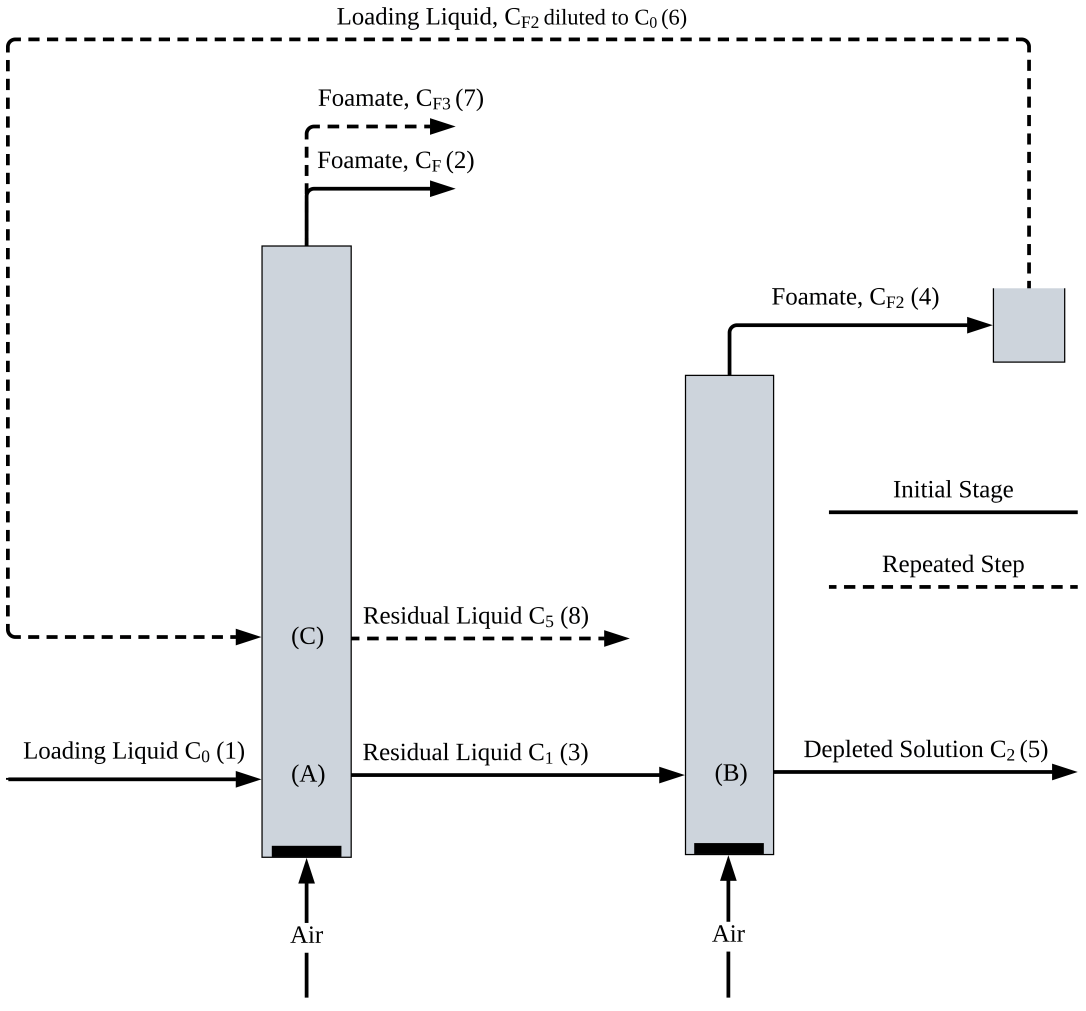

Figure 9. Diagram of two-stage foam fractionation method of saponin enrichment and recovery.

Table 2. Results of initial saponin concentration and volumetric air flow rate screening.

No.	Screened process variables		Resulting performance		
	C_0 [mg/cm^3]	Q [dm^3/h]	C_f [mg/cm^3]	E	R [%]
1	0.160	15	1.04 ± 0.05	6.49 ± 0.34	35.79 ± 1.85
2	0.320	10	0.95 ± 0.01	2.96 ± 0.01	28.59 ± 0.09
3	0.320	5	1.07 ± 0.01	3.36 ± 0.04	22.55 ± 0.24
4	0.160	10	1.16 ± 0.05	7.26 ± 0.31	23.33 ± 1.01
5	0.160	5	1.34 ± 0.04	8.41 ± 0.25	22.59 ± 0.68
6	0.064	10	1.30 ± 0.04	20.38 ± 0.63	15.86 ± 0.49

Table 3. Results of foam and liquid height screening.

No.	Screened process variables		Resulting performance		
	H_f [cm]	L_v [cm^3]	C_f [mg/cm^3]	E	R [%]
9	75	500	1.30 ± 0.04	20.38 ± 0.63	15.86 ± 0.49
10	65	700	0.81 ± 0.09	12.64 ± 1.38	16.67 ± 2.55
11	65	500	1.54 ± 0.04	24.16 ± 0.60	10.73 ± 0.27
13	55	500	1.66 ± 0.02	26.03 ± 0.36	7.24 ± 0.10
14	45	500	2.59 ± 0.02	40.56 ± 0.27	12.41 ± 0.08
15	35	500	2.39 ± 0.00	37.32 ± 0.04	15.75 ± 0.02

3.2.2. Simplex screening of the second stage

The first stage depleted the initial solution from 0.064 mg/cm^3 to 0.054 mg/cm^3 saponin content. A second stage was designed to concentrate the residual solution and reuse it in the first stage, hence the second stage process parameters were screened to improve saponin recovery percentage. Screening of sparger pore size and volumetric air flow rate was performed under initial saponin concentration of 0.054 mg/cm^3, total column height of 50 cm, loading liquid volume of 500 cm^3, natural pH and 25 ± 1 °C temperature.

According to Table 4, the second step screening showed improvement of recovery rate with increasing volumetric air flow rate and decreasing sparger pore size. Smaller pore sizes allow the production of more stable foams due to enhanced adsorption. Higher foam liquid fraction provides increasing recovery percentage of saponins, which also results from the increased amount of bubbles produced with increasing volumetric air flow rate. The recovery percentage increased from 45.44% to 70.64%, while maintaining decent enrichment ratio of 10.41. Volumetric air flow rate of 50 dm^3/h and 180 µm sparger pore size were chosen as optimal. Further increase in foamate

Table 4. Results of pore size and volumetric air flow rate screening.

No.	Screened process variables		Resulting performance		
	ϕ [μm]	Q [dm^3/h]	C_f [mg/cm^3]	E	R [%]
16	300	30	2.07 ± 0.07	38.06 ± 1.23	45.44 ± 1.47
17	300	40	0.67 ± 0.02	12.39 ± 0.33	55.00 ± 1.48
18	450	40	0.98 ± 0.04	18.09 ± 0.79	50.54 ± 2.21
19	230	40	0.69 ± 0.01	12.68 ± 0.15	64.81 ± 0.79
20	450	50	0.91 ± 0.03	16.76 ± 0.50	54.36 ± 1.64
21	300	50	0.71 ± 0.02	13.03 ± 0.41	64.26 ± 2.01
22	230	50	0.67 ± 0.05	12.29 ± 1.01	69.29 ± 5.67
23	180	40	0.59 ± 0.01	10.78 ± 0.20	67.05 ± 1.22
24	180	50	0.57 ± 0.02	10.41 ± 0.37	70.64 ± 2.51
25	230	60	0.48 ± 0.01	8.76 ± 0.23	65.27 ± 1.69

volume did not improve recovery percentage due to rapid reduction in saponin enrichment ratio probably resulting from insufficient bubble residence time in the liquid phase. The second stage improved depleted saponin concentration from 0.054 to 0.57 mg/cm^3. The foamate can be diluted and reused in the first stage in two-stage foam fractionation method.

3.2.3. Two-stage mode method

The two-stage batch mode was carried out, where the foaming liquid was depleted in the first column functioning as an enriching stage (A). Then the liquid was transferred to the second column functioning as a recovering stage (B), where the depleted solution was concentrated in the foamate. The second stage foamate was diluted, returned to the first stage to reuse the liquid and enrich it once again (C) as shown in Fig. 9. Operational parameters were set based on the screening results of the first and second stages. The results of two-stage mode simulation are shown in Table 5 with the highlighted streams.

As shown, two-stage batch technology improves overall recovery of saponin solution, while ensuring a high product enrichment ratio. Enrichment ratio in the first stage reaches nearly 50-fold increase in saponin concentration from 0.064 to 3.008 mg/cm^3 at 16.00% recovery. The remaining residual saponins were transferred to the second stage and recovered at 64.59% and moderate enrichment ratio of 12.63. The recyclate was reused and enriched in the second stage to achieve even greater enrichment ratio of over 100-fold, probably due to the depletion of more surface-active species from the initial solution. Lower surface activity of the recyclate resulted in less stable foam, thus greater enrichment. The two-stage cycle improved the total recovery rate of saponins in comparison to single stage alone from 16.60% to 71.63%. The residual solution of 0.031 mg/cm^3 saponin concentration may still be re-enriched and recycled. However, this process would be much more efficient in a continuous multi-stage mode manner where steady state could be achieved.

The results show higher performance in both the first and second stage compared to previous studies in this area (Jiang et al., 2016; Li et al., 2013; Yan et al., 2012). One of the reasons for this is attributed to the use of the resin that creates a hydrophobic surface for the printed columns. The result is enhanced foam drainage and the occurrence of enhanced internal reflux of interstitial fluid. The internal reflux ensures the establishment of a new equilibrium state of saponin adsorption.

3.3. Product analysis

3.3.1. FT-IR spectroscopy

The product from the first stage was analyzed using FT-IR Spectroscopy with reference to oleanolic acid triterpenoid genin. The characteristic infrared bands are distinguished in Fig. 10.

There are similarities among the two spectra due to the analogous structure of oleanolic acid and genins present in the sample. In the range of 3600–3000 cm^{-1}, vibrations of several overlapping functional groups are present, mainly O-H stretching vibrations. Saponins include hydroxylic or acidic groupings in their structure (mostly from sugar chains), therefore a stronger signal in comparison to oleanolic acid. Another band of 3000–2800 cm^{-1} belongs to the C–H stretching vibrations of hydrocarbons. The 1800–1500 cm^{-1} region consists of smaller bands with distinct differences in intensity, belonging to stretching vibrations of C=O groups and C=C groups. The last interval of 1500–1000 cm^{-1} corresponds to several overlapping bands. In this area, mainly C–H bending bonds of hydrocarbons and slightly lower O–H bending vibrations are distinguished. Bands below 1300 cm^{-1} indicate the presence of stretching vibrations belonging to C–O–C groupings strongly visible in the purified saponin sample. Below this range there is a dactyloscopic area carrying little structural information. The similarity of the two spectra and the visible stronger bands corresponding to the –OH, CH_2 and C–O–C groupings signal the presence of glycosides in the sample, where the triterpene backbone of oleanolic acid alone does not show these signals.

3.3.2. HPLC-UV analysis

The presence of glycosides was identified in the studied samples (Fig. 11). The obtained results are in agreement with the literature data, according to which they expose their presence in the initial stages of elution. The area between 1–5 minutes consists of small-molecule compounds viewed as impurities. From 5–15 minutes obtained signal corresponds to the presence of acyclic glycosides of sesquiterpene type. Signals occurring above 15 minutes correspond to cyclic glycosides including triterpenoid saponins (Ling et al., 2020; Murgu and Rodrigues-Filho, 2006; Shiau et al., 2009). Enriched saponin extract may contain both types of glycosides due to their

Table 5. Two-stage batch mode method results.

Stage No.	C_0 [mg/cm^3]	C_f [mg/cm^3]	E	R [%]
(A)	0.062 ± 0.000	3.008 ± 0.300	48.23 ± 4.81	16.00 ± 1.60
(B)	0.053 ± 0.001	0.663 ± 0.002	12.63 ± 0.04	66.07 ± 0.23
(C)	0.061 ± 0.004	7.043 ± 0.314	114.76 ± 5.12	35.58 ± 1.59

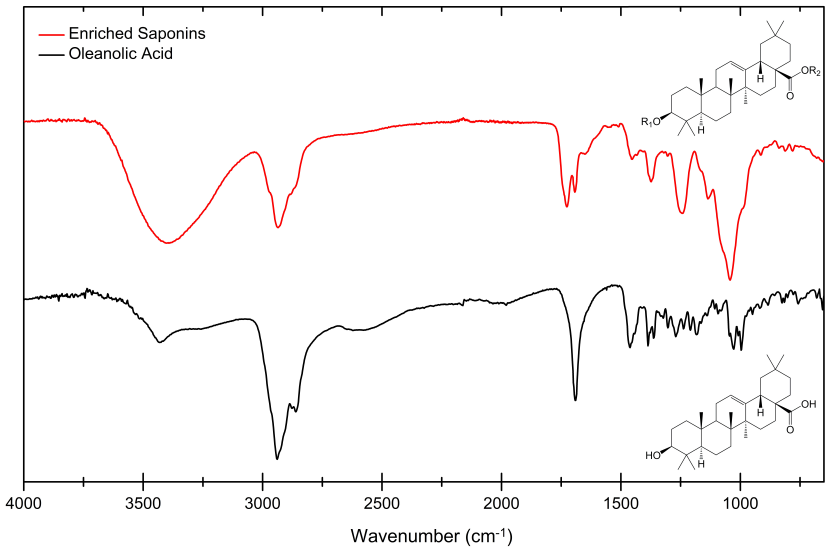

Figure 10. Foam fractionation product and oleanolic acid FT-IR Spectrum. The R_1 and R_2 substituents may represent a number of functional groups that belong to mono- and oligosaccharides. The complete list of potential combinations of substituents found in *S. mukorossi* saponins is available in previous publication (Sochacki and Vogt, 2022).

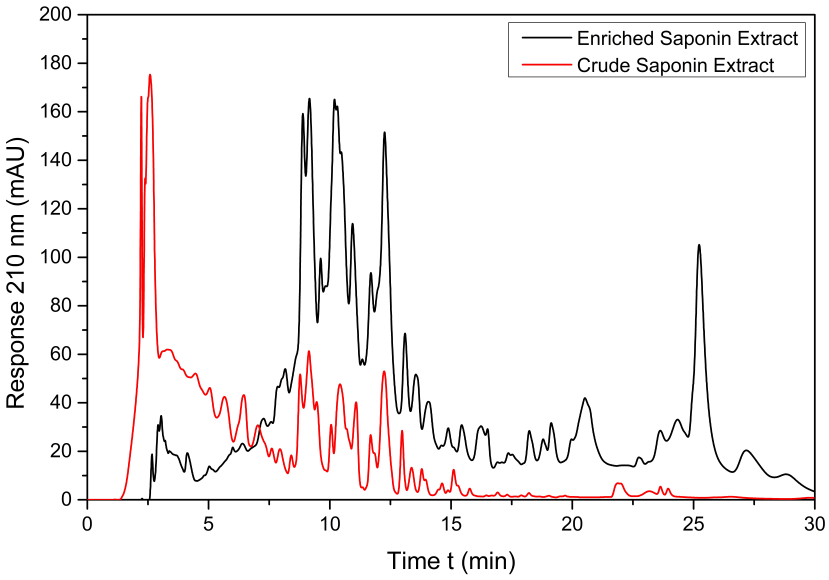

Figure 11. HPLC chromatograms of crude extract and enriched foamate detected at 210 nm.

surface activity and their transport within the foam. Foam fractionation enriched glycoside content, simultaneously reducing the content of low-molecular-weight compounds. Enrichment increased the content of trace compounds visible in the 15–25 minute range, which are not present in the crude extract.

4. CONCLUSIONS

The 3D printed column presented in the current work is suitable for the separation of plant biosurfactants through foam fractionation technology. High enrichment ratios can be obtained in single-stage mode reaching nearly 100-fold increase in saponin concentration with highly diluted saponin solutions. However, the single-stage mode does not allow for the separation of a significant amount of saponins from the solution due to low recovery. Introduction of a second column enriched the depleted solution from the first stage over 12-fold at suitable saponin percentage recovery of 66.07%. Under optimal operating conditions of two-stage mode the total saponin percentage recovery reached 71.63%.

3D printing technology is a simple and versatile tool for designing research equipment. Technology provides an easier way to modify printed components as required by ongoing analysis of research results. Despite that, it requires a good selection of printing material and equipment. In the case of Anycubic products during trials, limited quality, stability and

reproducibility of printing material was observed. Therefore, applicability of 3D printing for separation of saponins has been successful, but a better selection of printing materials would have improved the efficiency even further. It would be an improvement to choose a material with greater transparency, thermal and mechanical resistance. The process has potential industrial applications, but other printing solutions are required. At the current stage of research, the available equipment only allows for laboratory scale production.

The foam fractionation process is environmentally friendly because it uses water as the exclusive solvent and air as the carrier gas. Furthermore, the process itself does not generate additional waste. In fact, the process may be used to reduce the existing waste. In terms of energy, it is necessary to provide power for the air compressor. Power can be obtained from renewable energy sources. On the other hand, no additional chemical agents are used during foam separation.

ACKNOWLEDGMENTS

This research received no external funding support. The authors declare no conflict of interest.

REFERENCES

Arora J., Ranjan A., Chauhan A., Biswas R., Rajput V.D., Sushkova S., Mandzhieva S., Minkina T., Jindal T., 2022. Surfactant pollution, an emerging threat to ecosystem: approaches for effective bacterial degradation. *J. Appl. Microbiol.,* 133, 1229–1244. DOI: 10.1111/jam.15631.

Backleh-Sohrt M., Ekici P., Leupold G., Parlar H., 2005. Efficiency of foam fractionation for the enrichment of nonpolar compounds from aqueous extracts of plant materials. *J. Nat. Prod.,* 68, 1386–1389. DOI: 10.1021/np049743e.

Badmus S.O., Amusa H.K., Oyehan T.A., Saleh T.A., 2021. Environmental risks and toxicity of surfactants: overview of analysis, assessment, and remediation techniques. *Environ. Sci. Pollut. Res.,* 28, 62085–62104. DOI: 10.1007/s11356-021-16483-w.

Bartnik M., Facey P.C., 2017. Chapter 8 – Glycosides, In: Badal S., Delgoda R. (Eds.), *Pharmacognosy*. Academic Press, 101–161. DOI: 10.1016/B978-0-12-802104-0.00008-1.

Bhakta A., Ruckenstein E., 1997. Decay of standing foams: drainage, coalescence and collapse. *Adv. Colloid Interface Sci.,* 70, 1–124. DOI: 10.1016/S0001-8686(97)00031-6.

Bharadwaj T.K., Gupta K.N., 2021. Dye separation using a semi-batch foaming process: Process optimization using Taguchi methodology and Grey relational analysis. *Environ. Eng. Res.,* 26, 200242. DOI: 10.4491/eer.2020.242.

Boonyasuwat S., Chavadej S., Malakul P., Scamehorn J.F., 2003. Anionic and cationic surfactant recovery from water using a multistage foam fractionator. *Chem. Eng. J.,* 93, 241–252. DOI: 10.1016/S1385-8947(03)00043-3.

Buckley T., Xu X., Rudolph V., Firouzi M., Shukla P., 2022. Review of foam fractionation as a water treatment technology. *Sep. Sci. Technol.,* 57, 929–958. DOI: 10.1080/01496395.2021.1946698.

Burghoff B., 2012. Foam fractionation applications. *J. Biotechnol.,* 161, 126–137. DOI: 10.1016/j.jbiotec.2012.03.008.

Du L., Ding Y., Prokop A., Tanner R.D., 2001. Measurement of bubble size distribution in protein foam fractionation column using capillary probe with photoelectric sensors. In: Davison B.H., McMillan J., Finkelstein M. (Eds.), *Twenty-Second Symposium on Biotechnology for Fuels and Chemicals.* ABAB Symposium. Humana Press, Totowa, NJ., 91, 387–404. DOI: 10.1007/978-1-4612-0217-2_33.

Farn R.J., 2006. *Chemistry and technology of surfactants*. 1st edition, Wiley-Blackwell. DOI: 10.1002/9780470988596.

Hayes D.G., Smith G.A., 2019. Chapter 1 – Biobased surfactants: overview and industrial state of the art, In: Hayes D.G., Solaiman D.K.Y., Ashby R.D. (Eds.), *Biobased surfactants (Second Edition)*. AOCS Press, 3–38. DOI: 10.1016/B978-0-12-812705-6.00001-0.

Heng W., Ling Z., Na W., Youzhi G., Zhen W., Zhiyong S., Deping X., Yunfei X., Weirong Y., 2014. Analysis of the bioactive components of *Sapindus saponins*. *Ind. Crops Prod.,* 61, 422–429. DOI: 10.1016/j.indcrop.2014.07.026.

Hiai S., Oura H., Nakajima T., 1976. Color reaction of some sapogenins and saponins with vanillin and sulfuric acid. *Planta Med.,* 29, 116–122. DOI: 10.1055/s-0028-1097639.

Hojnik J., Ruzzier M., Konečnik Ruzzier M., 2019. Transition towards sustainability: adoption of eco-products among consumers. *Sustainability,* 11, 4308. DOI: 10.3390/su11164308.

Ivanković T., Hrenović J., 2010. Surfactants in the environment. *Arch. Ind. Hyg. Toxicol.,* 61, 95–110. DOI: 10.2478/10004-1254-61-2010-1943.

Jiang J., Wu Z., Liu W., Gao Y., Guo S., Kang S., 2016. Separation of soybean saponins from soybean meal by a technology of foam fractionation and resin adsorption. *Prep. Biochem. Biotechnol.,* 46, 346–353. DOI: 10.1080/10826068.2015.1031394.

Kaczerewska O., Martins R., Figueiredo J., Loureiro S., Tedim J., 2020. Environmental behaviour and ecotoxicity of cationic surfactants towards marine organisms. *J. Hazard. Mater.,* 392, 122299. DOI: 10.1016/j.jhazmat.2020.122299.

Khan R.A., 2018. Natural products chemistry: the emerging trends and prospective goals. *Saudi Pharm. J.,* 26, 739–753. DOI: 10.1016/j.jsps.2018.02.015.

Kharissova O.V., Kharisov B.I., Oliva González C.M., Peña Méndez Y., López I., 2019. Greener synthesis of chemical compounds and materials. *R. Soc. Open Sci.,* 6, 191378. DOI: 10.1098/rsos.191378.

Kumar A.K., Ghosh P., 2022. Removal and recovery of an anionic surfactant in the presence of alcohol by foam fractionation. *Ind. Eng. Chem. Res.,* 61, 7349–7360. DOI: 10.1021/acs.iecr.2c00372.

Kumar Dutta A., 2019. Introductory Chapter: Surfactants in household and personal care formulations - An overview, In: *Surfactants and detergents*. IntechOpen, 1–10. DOI: 10.5772/intechopen.89245.

Le A.V., Parks S.E., Nguyen M.H., Roach P.D., 2018. Improving the vanillin-sulphuric acid method for quantifying total saponins. *Technologies,* 6, 84. DOI: 10.3390/technologies6030084.

Lemlich R., 1968. Adsorptive bubble separation methods – Foam fractionation and allied techniques. *Ind. Eng. Chem.,* 60, 16–29. DOI: 10.1021/ie50706a005.

Lemlich R., 1972. *Adsorptive bubble separation techniques*. Academic Press. DOI: 10.1016/B978-0-12-443350-2.X5001-1.

Li L., Zhang Y., Wu Z., Liu Y., Zhang L., 2014. Separation of SDS from its determined lowest concentration by a two-stage foam separation. *Sep. Purif. Technol.,* 129, 50–56. DOI: 10.1016/j.seppur.2014.03.024.

Li R., Wu Z.L., Wang Y.J., Li L.L., 2013. Separation of total saponins from the pericarp of *Sapindus mukorossi* Gaerten. by foam fractionation. *Ind. Crops Prod.,* 51, 163–170. DOI: 10.1016/j.indcrop.2013.08.079.

Ling Y., Zhang Q., Zhong W., Chen M., Gong H., He S., Liang R., Lv J., Song L., 2020. Rapid identification and analysis of the major chemical constituents from the fruits of *Sapindus mukorossi* by HPLC-ESI-QTOF-MS/MS. *Nat. Prod. Res.,* 34, 2144–2150. DOI: 10.1080/14786419.2019.1577837.

Majinda R.R.T., 2012. Extraction and isolation of saponins. *Methods Mol. Biol.,* 864, 415–426. DOI: 10.1007/978-1-61779-624-1_16.

Moradpour N., Yang J., Tsai P.A., 2024. Liquid foam: fundamentals, rheology, and applications of foam displacement in porous structures. *Curr. Opin. Colloid Interface Sci.,* 74, 101845. DOI: 10.1016/j.cocis.2024.101845.

Morgan G., Wiesmann U., 2001. Single and multistage foam fractionation of rinse water with alkyl ethoxylate surfactants. *Sep. Sci. Technol.,* 36, 2247–2263. DOI: 10.1081/SS-100105916.

Moses T., Papadopoulou K.K., Osbourn A., 2014. Metabolic and functional diversity of saponins, biosynthetic intermediates and semi-synthetic derivatives. *Crit. Rev. Biochem. Mol. Biol.,* 49, 439–462. DOI: 10.3109/10409238.2014.953628.

Murgu M., Rodrigues-Filho E., 2006. Dereplication of glycosides from Sapindus saponaria using liquid chromatography-mass spectrometry. *J. Braz. Chem. Soc.,* 17, 1281–1290. DOI: 10.1590/S0103-50532006000700013.

Myers D., 2020. *Surfactant science and technology*. 4th edition, John Wiley & Sons, Inc., Hoboken, NJ, USA. DOI: 10.1002/9781119465829.

Sarachat T., Pornsunthorntawee O., Chavadej S., Rujiravanit R., 2010. Purification and concentration of a rhamnolipid biosurfactant produced by *Pseudomonas aeruginosa* SP4 using foam fractionation. *Bioresour. Technol.,* 101, 324–330. DOI: 10.1016/j.biortech.2009.08.012.

Shaban S.M., Kang J., Kim D.-H., 2020. Surfactants: recent advances and their applications. *Compos. Commun.,* 22, 100537. DOI: 10.1016/j.coco.2020.100537.

Shiau I.-L., Shih T.-L., Wang Y.-N., Chen H.-T., Lan H.-F., Lin H.C., Yang B.-Y., Ko C.-H., Murase Y., 2009. Quantification for saponin from a soapberry (Sapindus mukorossi Gaertn) in cleaning products by a chromatographic and two colorimetric assays. *J. Fac. Agric. Kyushu Univ.,* 54, 215–221. DOI: 10.5109/14063.

Sochacki M., Michorczyk P., Vogt O., 2025. Foam fractionation as an efficient method for the separation and recovery of surfactants and surface-inactive agents: state of the art. *ACS Omega,* 10, 55–75. DOI: 10.1021/acsomega.4c08413.

Sochacki M., Vogt O., 2022. Triterpenoid saponins from Washnut (*Sapindus mukorossi* Gaertn.)—A source of natural surfactants and other active components. *Plants,* 11, 2355. DOI: 10.3390/plants11182355.

Srinet S.S., Basak A., Ghosh P., Chatterjee J., 2017. Separation of anionic surfactant in paste form from its aqueous solutions using foam fractionation. *J. Environ. Chem. Eng.,* 5, 1586–1598. DOI: 10.1016/j.jece.2017.02.008.

Stevenson P., 2012. *Foam engineering: Fundamentals and applications*. Wiley-Blackwell. DOI: 10.1002/9781119954620.

Stevenson P., Li X., 2014. *Foam fractionation: Principles and process design*. CRC Press, Boca Raton. DOI: 10.1201/b16483.

Stochmal A., Oleszek W., Kapusta I., 2008. TLC of Triterpenes (Including Saponins), In: Waksmundzka-Hajnos M., Sherma J., Kowalska T. (Eds.), *Thin layer chromatography in phytochemistry*. CRC Press, Boca Raton, 519–537. DOI: 10.1201/9781420046786.

Tharapiwattananon N., Scamehorn J.F., Osuwan S., Harwell J.H., Haller K.J., 1996. Surfactant recovery from water using foam fractionation. *Sep. Sci. Technol.,* 31, 1233–1258. DOI: 10.1080/01496399608006948.

Wang Z., Zhang W., Gan W., Nie S., Gao H., Song L., 2022. Preparation of dioscin from *Trigonella foenum-graecum* by foam separation–preparative high-performance liquid chromatography. *Eur. Food Res. Technol.,* 248, 477–483. DOI: 10.1007/s00217-021-03893-w.

Wheaton F.W., Lawson T.B., Lomax K.M., 1979. Foam fractionation applied to aquacultural systems. *Proc. World Mariculture Society,* 10, 795–808. DOI: 10.1111/j.1749-7345.1979.tb00079.x.

Yan J., Wu Z., Wang W., 2012. Separation of tea saponin by two-stage continuous foam fractionation. *Sep. Sci. Technol.,* 47, 2460–2466. DOI: 10.1080/01496395.2012.666611.

Yan J., Wu Z., Zhao Y., Jiang C., 2011. Separation of tea saponin by two-stage foam fractionation. *Sep. Purif. Technol.,* 80, 300–305. DOI: 10.1016/j.seppur.2011.05.010.

Yang Q.-W., Wu Z.-L., Zhao Y.-L., Wang Y., Li R., 2011. Enhancing foam drainage using foam fractionation column with spiral internal for separation of sodium dodecyl sulfate. *J. Hazard. Mater.,* 192, 1900–1904. DOI: 10.1016/j.jhazmat.2011.07.018.